Rational design, synthesis, and photophysics of dual-emissive deoxyadenosine analogs

Hoang-Ngoan Le, Caterina Zilio, Guillaume Barnoin, Nicolas P.F. Barthes, Jean-Marie Guigonis, Nadine Martinet, Benoît Y. Michel, Alain Burger

Dyes and Pigments
journal homepage: www.elsevier.com

Rational design, synthesis, and photophysics of dual-emissive deoxyadenosine analogs

Hoang-Ngoan Le [a,†], Caterina Zilio [a], Guillaume Barnoin [a], Nicolas P.F. Barthes [a], Jean-Marie Guigonis [b], Nadine Martinet [a], Benoît Y. Michel,[a,*] Alain Burger [a,*]

[a] *Université Côte d'Azur, CNRS, Institut de Chimie de Nice, UMR 7272 – Parc Valrose, 06108 Nice cedex 2, France*
[b] *Université de Nice Sophia Antipolis, Faculté de Médecine, Plateforme "Bernard Rossi", Nice, France*
[†] *Main contributor to these research works*

ARTICLE INFO

Article history:
Received
Received in revised form
Accepted
Available online

Keywords:
Nucleoside Analogs
3-HydroxyChromone
Dual Emission
Push–Pull Dye
Solvent Polarity

ABSTRACT

Dual-emissive deoxyadenosine analogs were engineered by compiling 7-deaza-7-ethynyl-2'-deoxyadenosine with two-color dyes, 3-HydroxyChromones (3HC), while electronically conjugating the *N*9-donor of the nucleobase with the 3HC carbonyl. Their spectroscopic properties were investigated in a set of solvents of different polarities. Several improvements in the 3HC photophysical features were obtained. A significant bathochromic shift moved absorption to the visible range, the extinction coefficient was almost doubled and the fluorescence emission displayed a mega-Stokes shift of the tautomer emission band (>175 nm). The ratio intensity of the dual emission demonstrated high sensitivity to polarity changes, offering a well-resolved green-yellow emission. Considering the strong donating ability of the *N*9, angular and reversed assemblies were also considered in order to tune the photophysics by weakening the excited-state dipole moment.

1. Introduction

Nucleosides constitute the critical building blocks of nucleic acids [1]. Redesigning their structure and incorporating the resulting nucleoside analog into oligonucleotides is a conventional approach to produce modified DNA sequences for chemical biology purposes [2]. Changes that make DNA fluorescent is a dominant technique, thanks to the non-invasive character and high sensitivity of response of fluorescence spectroscopy [3,4]. Due to their low intrinsic fluorescence, the four DNA nucleobases cannot be used to report biological events, as can be achieved in proteins with the help of Trp residues [5-9]. Thus modification of the nucleobase structure is one attractive option, to improve analyses of nucleic acids. This requires changing of the π-system or connecting of a fluorescent moiety [10]. Whichever strategy is chosen, the development of fluorophores that perfectly satisfy the demanding specification (such as the sensitivity to environment variations and interactions, the brightness, the compatibility with available laser lines for excitation to name a few) turns out to be an extremely complex task [11,12]. In this context, we have investigated the synthesis of advanced emissive nucleosides as responsive new sensors for the local hydrated environment of DNA, since structural changes and interactions with proteins and other ligands impact the proximal water distribution and polarity around the DNA [13]. These fluorophores are based on a 3-HydroxyChromone (3HC) scaffold and present dual emission, i.e. emission with two distinct colors. Indeed, through an excited-state intramolecular proton transfer (ESIPT reaction), these dyes have the unique ability to display two tautomer forms, emitting separately to each other at two well-defined wavelengths (green and yellow, N* and T* bands respectively, *Scheme 1*)[14-17].

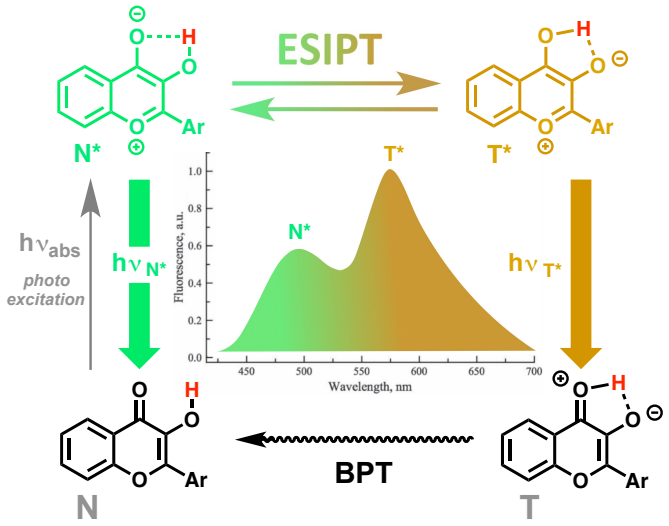

Scheme 1. ESIPT reaction: origin of the dual emissions for 3HC fluorophores leading to a two-color response for sensing polarity changes. *BPT denotes Back Proton Transfer*.

3HCs proved to be extremely sensitive to proximal disturbances, as reflected by a considerable change in the intensity ratio of the two emission bands, and hence by a readily

quantifiable change in color [18-21]. We first investigated internal DNA labeling by nucleobase replacement with 3HC fluorophores [22,23]. DNA sequences site-specifically tagged according to this strategy were applied to the mechanistic studies of DNA repair and methylation [24,25] as well as for HIV-1 replication [26]. These examples of a fluorescence-based approach attested the outstanding sensitivity of this nucleobase surrogate to structural changes accompanying protein binding and base flipping, while the structure of the duplex and its protein affinity were only marginally affected. Minimal DNA perturbation by the dye incorporation was further supported by NMR investigations [27].

Although these prospective probes helped overcome several bottlenecks encountered in nucleic acids labeled with commonly used fluorophores such as 2-aminopurine, their sensitivity to hydration changes was not optimal. Recently, we engineered efficient synthetic access to the DNA major groove labeling by electronically compiling 3HC fluorophores to a uracil moiety (*Figure 1, left*)[13,28,29]. These fluorescent deoxyuridine analogs demonstrated exquisite sensitivity to hydration via two distinct sources: the wide variation of the intensity ratio of the two emission bands (*Figure S1, arrow A*) and the hypsochromic shift of the T* form (*arrow B*)[13]. This multiparametric sensing mechanism appears to be completely unique since it presents the decisive advantage to precisely monitor subtle local changes of hydration – independently of the probe concentration or the fluctuations of the fluorometer being used – by simultaneously exploiting the two channels of fluorescence (*Figure S1*).[29]

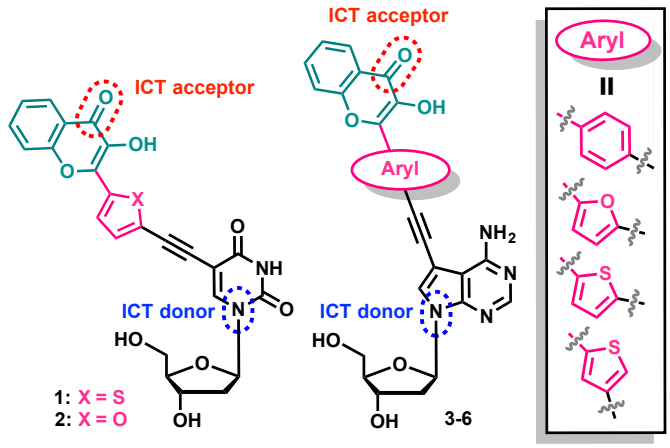

Figure 1. Nucleoside labeling strategy – *Modification of a natural base:* structures of the 3HC-engineered dU (*left*, reported) [13,28,29] and dA analogs (*right*, present work). *ICT denotes Intramolecular Charge Transfer.*

In the continuation of this work, we sought to complete our ratiometric toolbox of fluorescent nucleoside analogs to the purine series by preparing dA analogs presenting 2-aryl substituents with different donating abilities. Final targets **3–5**, namely **PCA**, **FCA**, **TCA** (P = phenyl, F = furyl, T = thienyl, C = 3HC, *Figures 1&2*), were rationally designed in such a way that the *N*9 position is electronically conjugated to the ketone of the flavonoid C ring to establish an extended D-π-A push–pull system (D = donor, A = acceptor) and to favor intramolecular charge transfer (ICT; *Figure 1, right*).

Hence, these two-color nucleoside analogs were expected to have a strong push–pull character in the excited state [30,31]. To modulate the latter, two different molecular architectures were also explored. One involves a 2,4-disubstituted thienyl isomer while the other presents a dipole moment attenuated due to a reversed connectivity orientation (**angTCA 6** and **revTCA 7**, ang = angular, and rev = reversed, *Figures 1&2*). Herein, we report the synthesis of the five 3HC-based dA analogs by a convergent approach. To this end, the final assembly between 7-deaza-7-ethynyl-dA and 3HC parent dyes with various electronic features is performed by a Sonogashira coupling under mild conditions. A photophysical characterization of each dual-emissive dA analog is described for a set of 10 solvents with increasing polarity. Correlations between spectroscopic properties, polarity parameters and the strength of the push–pull character are discussed to discriminate and select the most promising analogs for a further oligodeoxynucleotide (ODN) incorporation.

2. Experimental section

2.1. General Procedures – Materials and Methods

All reactions involving air- and water-sensitive conditions were performed in oven-dried glassware under argon by using Schlenk techniques employing a dual vacuum/argon manifold system and dry solvents. The synthetic intermediates were initially co-evaporated twice with toluene and dried *in vacuo* before use. All chemical reagents were purchased from commercial sources (Sigma-Aldrich, Acros, Alfa Aesar) and were used as supplied. Anhydrous solvents were obtained according to standard procedures [32]. The reactions were monitored simultaneously by liquid chromatography–mass spectrometry (LC-MS) and thin-layer chromatography (TLC, silica gel 60 F254 plates). Compounds were visualized on TLC plates by both UV radiation (254 and 365 nm) and spraying with a staining agent (Vanillin, PMA, $KMnO_4$ or ninhydrin)[33] followed by subsequent warming with a heat gun.

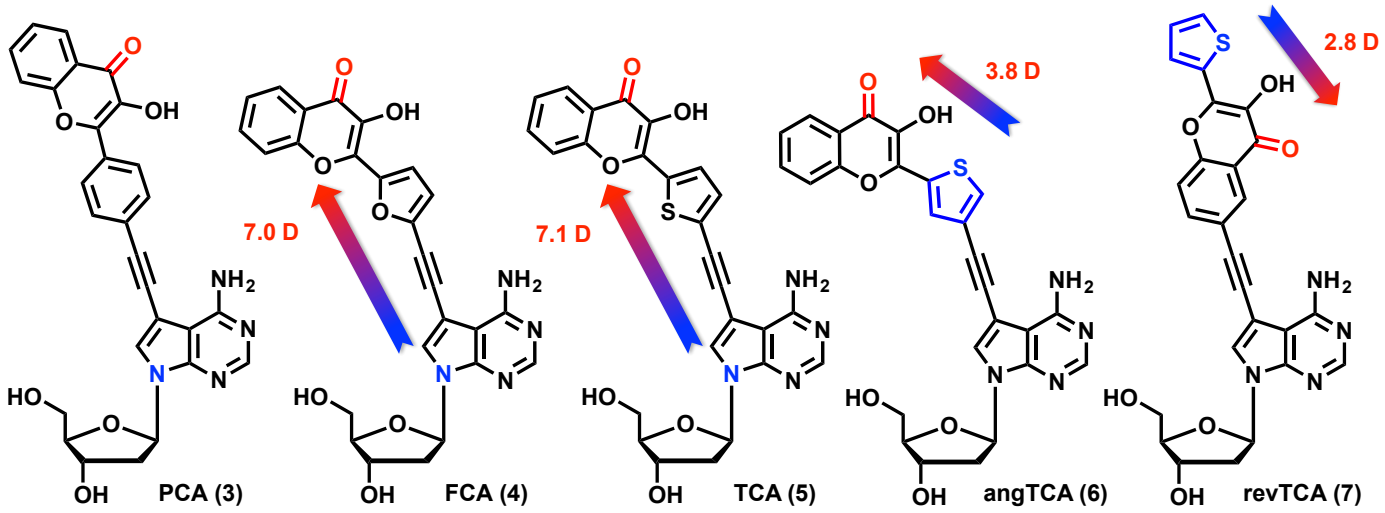

Figure 2. Dual-emissive dA analogs investigated in this study. *Donor and acceptor groups are depicted in blue and red, respectively. Gradient colored arrows represent the D-π-A push–pull system. The differences in the dipole moments of excited and ground states – given in Debye (D) – were obtained according to the Lippert–Mataga model (Part S2). The length of the arrow reflects the magnitude of the difference.*

Column chromatography was performed with flash silica gel (40−63 μm) with the indicated solvent system using gradients of increasing polarity in most cases [34]. All NMR spectra (^{1}H, ^{13}C, ^{2}D) were recorded on 200, 400 or 500 MHz Bruker Advance Spectrometers. ^{1}H-NMR (200, 400 and 500 MHz) and ^{13}C{^{1}H}NMR (50, 101 and 126 MHz, recorded with complete proton decoupling) spectra were obtained with samples dissolved in $CDCl_3$, CD_2Cl_2, CD_3OD, DMSO-d^6, acetone-d^6, CD_3CN or C_5D_5N with the residual solvent signals used as internal references: 7.26 ppm for C*H*Cl_3, 5.32 ppm for CD*H*Cl_2, 3.31 ppm for CD_2*H*OD, 2.50 ppm for (CD_3)(CD_2*H*)S(O), 2.05 ppm for (CD_3)(CD_2*H*)C(O), 1.94 ppm for CD_2*H*CN, 8.74 ppm for C_5D_4*H*N regarding ^{1}H-NMR experiments, and 77.2 ppm for $CDCl_3$, 53.8 ppm for CD_2Cl_2, 49.0 ppm for CD_3OD, 39.4 ppm for $(CD_3)_2S(O)$, 30.8 ppm for $(CD_3)_2C(O)$, 118.7 ppm for CD_3CN, 150.3 ppm for C_5D_5N concerning ^{13}C-NMR experiments [35,36]. Chemical shifts (δ) are given in ppm to the nearest 0.01 (^{1}H) or 0.1 ppm (^{13}C). The coupling constants (*J*) are given in Hertz (Hz). The signals are reported as follows: (s = singlet, d = doublet, t = triplet, m = multiplet, br = broad). Assignments of ^{1}H and ^{13}C NMR signals were achieved with the help of D/H exchange, COSY, DEPT, APT, HMQC, HSQC, TOCSY, NOESY, and HMBC experiments. LC-MS spectra were recorded using an ion trap Esquire 3000 Plus mass spectrometer equipped with an electrospray ionization (ESI) source in both positive and negative modes. High-resolution mass spectrometry (HRMS) was conducted with a hybrid ion trap−Orbitrap mass spectrometer (combining quadrupole precursor selection with high-resolution and accurate-mass Orbitrap detection) using ESI techniques. Systematic flavone and nucleobase nomenclatures are used below for the assignment of each spectrum. All solvents for absorption and fluorescence experiments were of spectroscopic grade. Absorption spectra were recorded on a Cary 100 Bio UV–Vis spectrophotometer (Varian/Agilent) using Suprasil® quartz cuvettes with 1 cm path length. Stock solutions of dyes **3–7** were prepared using dimethylformamide. The samples used for spectroscopic measurements contained ≈ 0.2 % v/v of solvents of the stock solution. Fluorescence spectra were recorded on a FluoroMax 4.0 spectrofluorometer (Jobin Yvon, Horiba) with a thermostated cell compartment at 20 ± 0.5 °C with slits open to 2 nm and were corrected for Raman scattering, lamp fluctuations and instrumental wavelength-dependent bias. Excitation wavelength was used as described in the corresponding experiments.

2.2. Synthesis

2.2.1. **6-Chloro-7-deaza-2′-deoxy-7-iodo-3′,5′-di-*O*-*p*-toluoyladenosine**[37] **(9):** To a stirred suspension of KOH (250 mg, 2.5 eq) in dry CH_3CN (36 mL; previously sonicated over 1 min), were successively added TDA-1 (47 μL, 0.07 eq) and 6-chloro-7-deaza-7-iodopurine (500 mg, 1.79 mmol). The resulting solution was stirred at room temperature (rt) for 10 min, until the suspension became clearer. Hoffer's sugar **8** (850 mg, 1.2 eq) was added half at a time over 2 min and stirring was maintained for 10 min. The reaction mixture was diluted with CH_2Cl_2 (10 mL) and then the insoluble material was filtered and washed with CH_2Cl_2 (2 x 20 mL). The volatiles were removed under reduced pressure and the residue was purified by flash chromatography on silica gel eluted with toluene/EtOAc (1:0 → 4:1, v/v) to provide the desired product **9** as a white foam (860 mg, 76 %). $C_{27}H_{23}ClIN_3O_5$ (631.85). R_f = 0.6 (toluene/EtOAc = 85:15); R_f = 0.5 (PE/EtOAc = 7:3). ^{1}H-NMR (200 MHz, $CDCl_3$): δ 8.61 (s, 1H), 8.20–7.79 (m, 4H), 7.57 (s, 1H), 7.40–7.15 (m, 4H), 6.79 (t, *J* = 7.1 Hz, 1H), 5.75 (qd, *J* = 4.1, 2.1 Hz, 1H), 4.89–4.48 (m, 3H), 2.78 (dd, *J* = 7.1, 4.2 Hz, 2H), 2.45 (s, 3H), 2.43 (s, 3H). ^{13}C-NMR (50 MHz, $CDCl_3$): δ 166.3, 166.1, 153.0, 151.1, 150.7, 144.7, 144.4, 131.6, 130.0, 129.8, 129.6, 129.4, 126.7, 126.5, 117.7, 84.6, 83.0, 75.2, 64.1, 53.0, 38.6, 21.9. HRMS (ESI$^+$): *m/z* calcd for $C_{27}H_{24}ClIN_3O_5$: 632.0444 $[M+H]^+$; found 632.0434.

2.2.2. **7-Deaza-2′-deoxy-7-iodo-3′,5′-di-*O*-*p*-toluoyladenosine (10):** To a saturated solution of NH_3 in BuOH (3.5 M, 4 mL), **9** (500 mg, 0.79 mmol) was added. The reaction mixture was stirred under microwave irradiation at 150 °C (100 W, 100 psi) for 15 minutes. The volatiles were removed *in vacuo* and the resulting residue was purified by flash chromatography on silica gel eluted with toluene/EtOAc (1:9 → 55:45, v/v) to provide the desired compound **10** as a white solid (402 mg, 83 %). $C_{27}H_{25}IN_4O_5$ (612.42). R_f = 0.2 (PE/EtOAc = 1:1). ^{1}H-NMR (200 MHz, $CDCl_3$): δ 8.29 (s, 1H), 8.15–7.82 (m, 4H), 7.58–7.14 (m, 4H), 6.80 (t, *J* = 7.1 Hz, 1H), 6.04 (s, 2H), 5.75 (td, *J* = 4.2, 2.3 Hz, 1H), 4.88–4.51 (m, 3H), 2.75 (dd, *J* = 7.2, 4.2 Hz, 2H), 2.46 (s, 6H). ^{13}C-NMR (50 MHz, $CDCl_3$): δ 166.3, 166.1, 156.8, 151.9, 150.3, 144.6, 144.3, 129.9, 129.8, 129.5, 129.4, 126.9, 126.5, 125.9, 104.4, 84.0, 82.6, 75.3, 64.3, 51.6, 38.5, 21.9. MS (ESI$^+$, MeOH) *m/z*: 613.0 $[M+H]^+$. HRMS (ESI$^+$): *m/z* calcd for $C_{27}H_{26}IN_4O_5$: 613.0942 $[M+H]^+$; found 613.0947.

2.2.3. **7-Deaza-2′-deoxy-3′,5′-di-*O*-(*p*-toluoyl)-7-((trimethylsilyl)ethynyl)adenosine**[37] **(11):** To a stirred solution of **10** (940 mg, 1.5 mmol) in THF (31 mL) under argon, were sequentially added Et_3N (1.10 mL, 5 eq.), TMS-acetylene (330 μL, 1.5 eq.), and a mixture of CuI (8 mol%, 24 mg) / $PdCl_2(PPh_3)_2$ (8 mol%, 87 mg). The reaction mixture was stirred at 60 °C under argon for 2 h. Then, the resulting solution was diluted with CH_2Cl_2 (30 mL) and evaporated under reduced pressure. The residue was purified by flash chromatography on silica gel eluted with PE/EtOAc (9:1 → 4:6, v/v) to provide the desired compound **11** as a yellow foam (659 mg, 74 %). $C_{32}H_{34}N_4O_5Si$ (582.73). R_f = 0.5 (PE/EtOAc = 2:3). ^{1}H-NMR (500 MHz, CD_2Cl_2): δ 8.24 (s, 1H), 8.07–7.88 (m, 4H), 7.35 (s, 1H), 7.33–7.25 (m, 4H), 6.71 (dd, *J* = 8.2, 5.9 Hz, 1H), 5.93–5.52 (m, 3H), 4.66 (dd, *J* = 11.9, 4.1 Hz, 1H), 4.61 (dd, *J* = 11.9, 4.0 Hz, 1H), 4.56 (td, *J* = 4.1, 2.6 Hz, 1H), 2.80 (ddd, *J* = 14.5, 8.3, 6.4 Hz, 1H), 2.71 (ddd, *J* = 14.2, 5.9, 2.6 Hz, 1H), 2.43 (s, 3H), 2.42 (s, 3H), 0.26 (s, 9H). ^{13}C-NMR (126 MHz, CD_2Cl_2): δ 166.7, 166.5, 158.1, 153.8, 150.5, 145.1, 144.7, 130.3, 130.1, 129.8, 129.8, 127.5, 127.3, 126.0, 104.1, 98.7, 97.9, 97.1, 84.5, 82.9, 75.6, 64.8, 38.6, 22.0, 0.1. HRMS (ESI$^+$): *m/z* calcd for $C_{32}H_{35}N_4O_5Si$: 583.2371 $[M+H]^+$; found 583.2374.

2.2.4. **7-Deaza-2′-deoxy-7-ethynyladenosine**[37] **(12):** To a stirred solution of **11** (620 mg, 1.1 mmol) in CH_2Cl_2 (5 mL), a saturated solution of K_2CO_3 in MeOH (20 mL) was added. The reaction mixture was stirred for 2 h at rt. The volatiles were evaporated under reduced pressure and the resulting residue was purified by flash chromatography on silica gel eluted with CH_2Cl_2/MeOH (98:2 → 85:15, v/v) to provide the desired compound **12** as a white solid (260 mg, 89 %). $C_{13}H_{14}N_4O_3$ (274.28). R_f = 0.2 (CH_2Cl_2/MeOH = 9:1). ^{1}H-NMR (400 MHz, CD_2Cl_2 with drops of CD_3OD): δ 8.04 (s, 1H), 7.50 (s, 1H), 6.34 (dd, *J* = 8.3, 5.9 Hz, 1H), 4.45 (td, *J* = 5.4, 2.5 Hz, 1H), 3.96 (q, *J* = 3.0 Hz, 1H), 3.74 (dd, *J* = 12.2, 3.0 Hz, 1H), 3.65 (dd, *J* = 12.2, 3.2 Hz, 1H), 3.51 (s, 1H), 2.58 (ddd, *J* = 13.8, 8.3, 5.9 Hz, 1H), 2.24 (ddd, *J* = 13.6, 6.1, 2.6 Hz, 1H). ^{13}C-NMR (101 MHz, CD_2Cl_2 with drops of CD_3OD): δ 158.7, 152.8, 149.2, 128.8, 104.7, 95.7, 88.9, 87.1, 81.4, 77.3, 72.6, 63.3, 41.3. MS (ESI$^+$, MeOH) *m/z*: 275.0 $[M+H]^+$.

2.2.5. **7-Deaza-2′-deoxy-7-((4-(3-hydroxy-4-oxochromen-2-yl)phen-1-yl)ethynyl)adenosine (3 – PCA):** To a stirred solution of **12** (35 mg, 0.128 mmol) and **13** (81 mg, 1.3 eq.) in DMF (11 mL) that was previously degassed by sonication under argon, were sequentially added Et_3N (65 μL, 5 eq.), and a mixture of CuI (7 mol%, 2 mg) / $PdCl_2(PPh_3)_2$ (7 mol%, 6 mg). The reaction mixture was warmed to 60 °C under argon for 1 h. The resulting solution was diluted with CH_2Cl_2 (10

mL) and the volatiles were removed *in vacuo*. The residue was purified by flash chromatography on silica gel eluted with CH_2Cl_2/MeOH (98:2 → 85:15, v/v) to provide the coupled product as a yellow solid (50 mg, 61 %). R_f = 0.4 (CH_2Cl_2/MeOH = 9:1). MS (ESI^+, MeOH) *m/z*: 645.2 $[M+H]^+$. The latter was sufficiently pure to be engaged in the next step without further purification. To a stirred solution of this Cbz-protected intermediate (40 mg, 0.062 mmol) in DMF (2 mL), a saturated methanolic solution of NH_3 (ca. 9 M, 5 mL) was added. The reaction was stirred for 5 min at rt. The volatiles were removed *in vacuo* and the residue was purified by flash chromatography on silica gel eluted with $CHCl_3$/(mixture MeOH/H_2O 5:1, v/v) (100:0 → 90:10, v/v) to provide the desired product **3** as a yellow-orange solid (19 mg, 60 %). $C_{28}H_{22}N_4O_6$ (510.51). R_f = 0.3 (CH_2Cl_2/MeOH = 9:1); R_f = 0.6 ($CHCl_3$/MeOH/H_2O = 10:1:0.2). ^{1}H-NMR (500 MHz, DMF-d^7): δ 9.99 (s, 1H), 8.47–8.37 (m, 2H), 8.22 (s, 1H), 8.17 (dd, *J* = 8.0, 1.5 Hz, 1H), 8.06 (s, 1H), 7.88 (ddd, *J* = 8.3, 6.6, 1.6 Hz, 1H), 7.87–7.82 (m, 3H), 7.53 (ddd, *J* = 8.0, 6.6, 1.4 Hz, 1H), 6.87 (s, 2H), 6.68 (dd, *J* = 8.2, 5.9 Hz, 1H), 5.43 (d, *J* = 3.9 Hz, 1H), 5.36 (t, *J* = 5.7 Hz, 1H), 4.66–4.49 (m, 1H), 4.02 (td, *J* = 3.9, 2.3 Hz, 1H), 3.79 (dt, *J* = 11.8, 4.5 Hz, 1H), 3.73 (ddd, *J* = 11.8, 6.2, 3.8 Hz, 1H), 2.69 (ddd, *J* = 13.5, 8.2, 5.7 Hz, 1H), 2.38 (ddd, *J* = 13.1, 6.0, 2.6 Hz, 1H). ^{13}C-NMR (126 MHz, DMF-d^7): δ 174.4, 159.2, 156.2, 154.2, 151.0, 145.3, 134.9, 132.5, 132.3, 128.8, 128.6, 125.9, 125.7, 125.4, 122.6, 119.6, 103.7, 101.0, 96.1, 92.2, 89.5, 86.2, 85.4, 72.8, 63.7, 41.7. MS (ESI^+, MeOH) *m/z*: 510.9 $[M+H]^+$. HRMS (ESI^+): *m/z* calcd for $C_{28}H_{23}N_4O_6$: 511.1612 $[M+H]^+$; found 511.1623.

2.2.6. **7-Deaza-2′-deoxy-7-((5-(3-hydroxy-4-oxochromen-2-yl)furan-2-yl)ethynyl)adenosine (4 – FCA):** To a stirred solution of **12** (60 mg, 0.22 mmol) and **14** (122 mg, 1.2 eq.) in DMF (11 mL), previously degassed by sonication under argon, were sequentially added Et_3N (152 μL, 5 eq.), and a mixture of CuI (7 mol%, 3 mg) / $PdCl_2(PPh_3)_2$ (7 mol%, 11 mg). The reaction mixture was warmed to 60 °C under argon for 1 h. The resulting solution was diluted with CH_2Cl_2 (20 mL) and the volatiles were removed *in vacuo*. The residue was purified by flash chromatography on silica gel eluted with CH_2Cl_2/MeOH (98:2 → 85:15, v/v) to provide the coupled product as a yellow-orange solid (120 mg, 86 %). R_f = 0.45 (CH_2Cl_2/MeOH = 9:1). MS (ESI^+, MeOH) *m/z*: 635.2 $[M+H]^+$. The latter was sufficiently pure to be used in the next step without further purification. To a stirred solution of this Cbz-protected intermediate (110 mg, 0.17 mmol) in DMF (1.5 mL), a saturated methanolic solution of NH_3 (ca. 9 M, 10 mL) was added. The reaction was stirred for 5 min at rt. The volatiles were removed *in vacuo* and the residue was purified by flash chromatography on silica gel eluted with CH_2Cl_2/MeOH (98:2 → 85:15, v/v) to provide the desired product **4** as an orange solid (30 mg, 35 %). $C_{26}H_{20}N_4O_7$ (500.47). R_f = 0.27 (CH_2Cl_2/MeOH = 9:1). ^{1}H-NMR (400 MHz, DMF-d^7): δ 10.50 (s, 1H), 8.24 (s, 1H), 8.17 (dd, *J* = 7.9, 1.6 Hz, 1H), 8.14 (s, 1H), 7.86 (ddd, *J* = 8.6, 7.0, 1.7 Hz, 1H), 7.77 (dd, *J* = 8.6, 1.0 Hz, 1H), 7.53 (ddd, *J* = 8.0, 7.0, 1.1 Hz, 1H), 7.47 (d, *J* = 3.7 Hz, 1H), 7.24 (d, *J* = 3.7 Hz, 1H), 6.92 (s, 2H), 6.69 (dd, *J* = 8.1, 5.9 Hz, 1H), 5.44 (d, *J* = 3.9 Hz, 1H), 5.36 (dd, *J* = 6.2, 5.1 Hz, 1H), 4.58 (qd, *J* = 5.8, 2.7 Hz, 1H), 4.03 (td, *J* = 3.9, 2.4 Hz, 1H), 3.80 (ddd, *J* = 11.8, 5.1, 4.0 Hz, 1H), 3.74 (ddd, *J* = 11.8, 6.2, 3.9 Hz, 1H), 2.69 (ddd, *J* = 13.5, 8.1, 5.7 Hz, 1H), 2.40 (ddd, *J* = 13.1, 6.0, 2.7 Hz, 1H). ^{13}C-NMR (101 MHz, DMF-d^7): δ 173.2, 159.1, 155.7, 154.3, 151.1, 146.5, 139.6, 139.5, 139.4, 134.9, 129.6, 126.0, 125.8, 123.3, 119.4, 119.4, 117.5, 103.6, 94.8, 90.7, 89.6, 85.5, 82.0, 72.8, 63.6, 41.8. HRMS (ESI^+): *m/z* calcd for $C_{26}H_{21}N_4O_7$: 501.1405 $[M+H]^+$; found 501.1408.

2.2.7. **7-Deaza-2′-deoxy-7-((5-(3-hydroxy-4-oxochromen-2-yl)thiophen-2-yl)ethynyl)adenosine (5 – TCA):** To a stirred solution of **12** (49 mg, 0.18 mmol) and chromone **15** (103 mg, 1.2 eq.) in DMF (4 mL), previously degassed by sonication under argon, were sequentially added Et_3N (125 μL, 5 eq.), and a mixture of CuI (7 mol%, 2 mg) / $PdCl_2(PPh_3)_2$ (7 mol%, 9 mg). The reaction mixture was warmed to 60 °C under argon for 1 h. The resulting solution was diluted with CH_2Cl_2 (10 mL) and the volatiles were removed *in vacuo*. The residue was purified by flash chromatography on silica gel eluted with CH_2Cl_2/MeOH (98:2 → 85:15, v/v) to provide the coupled product as a yellow-orange solid (78 mg, 67 %). R_f = 0.5 ($CHCl_3$/MeOH = 85:15). MS (ESI^+, MeOH) *m/z*: 651.2 $[M+H]^+$. The latter was sufficiently pure to be used in the next step without further purification. To a stirred solution of this Cbz-protected intermediate (78 mg, 0.17 mmol) in pyridine (1 mL) a 10% aq. NH_4OH solution in MeOH (10 mL) was added. The reaction mixture was stirred for 5 min at rt and quenched with acetic acid until pH = 4. Additional H_2O (20 mL) was introduced to initiate the precipitation. The resulting mixture was stored overnight at 0–5 °C. The heterogeneous mixture was centrifuged to settle solid particles and the supernatant was carefully removed by a syringe with a fine needle. The solid was washed with a solution of MeOH/H_2O (7:3), and after centrifugation, the supernatant was removed by suction. This washing procedure was repeated twice more to provide the desired product **5** as an orange solid (15 mg, 24 %). $C_{26}H_{20}N_4O_6S$ (516.53). R_f = 0.55 (acetone). ^{1}H-NMR (500 MHz, DMF-d^7): δ 10.94 (s, 1H), 8.23 (s, 1H), 8.15 (dd, *J* = 8.0, 1.6 Hz, 1H), 8.08 (s, 1H), 7.98 (d, *J* = 4.0 Hz, 1H), 7.86 (ddd, *J* = 8.6, 7.0, 1.7 Hz, 1H), 7.79 (d, *J* = 8.2 Hz, 1H), 7.65 (d, *J* = 4.0 Hz, 1H), 7.52 (ddd, *J* = 8.0, 6.9, 1.1 Hz, 1H), 6.90 (s, 2H), 6.68 (dd, *J* = 8.1, 5.9 Hz, 1H), 4.61–4.54 (m, 1H), 4.02 (td, *J* = 3.9, 2.3 Hz, 1H), 3.79 (dt, *J* = 11.8, 4.3 Hz, 1H), 3.73 (ddd, *J* = 11.8, 5.8, 3.8 Hz, 1H), 2.68 (ddd, *J* = 13.5, 8.2, 5.7 Hz, 1H), 2.38 (ddd, *J* = 13.1, 6.0, 2.6 Hz, 1H). ^{13}C-NMR (101 MHz, DMF-d^7): δ 172.6, 158.4, 155.1, 153.4, 150.4, 142.6, 134.1, 132.9, 128.4, 128.2, 127.0, 125.2, 124.9, 122.5, 118.5, 102.9, 95.0, 90.0, 88.8, 84.7, 84.4, 72.1, 62.9, 41.0. HRMS (ESI^+): *m/z* calcd for $C_{26}H_{21}N_4O_6S$: 517.1176 $[M+H]^+$; found 517.1178.

2.2.8. **7-Deaza-2′-deoxy-7-((5-(3-hydroxy-4-oxochromen-2-yl)thiophen-3-yl)ethynyl)adenosine (6 – angTCA):** To a stirred solution of **12** (59 mg, 0.215 mmol) and **16** (124 mg, 1.2 eq.) in DMF (11 mL), previously degassed by sonication under argon, were sequentially added Et_3N (150 μL, 5 eq.), and a mixture of CuI (7 mol%, 3 mg) / $PdCl_2(PPh_3)_2$ (7 mol%, 11 mg). The reaction mixture was warmed to 60 °C under argon for 1 h. The resulting solution was diluted with CH_2Cl_2 (10 mL) and the volatiles were removed *in vacuo*. The residue was purified by flash chromatography on silica gel eluted with CH_2Cl_2/MeOH (98:2 → 85:15, v/v) to provide the coupled product as a yellow solid (120 mg, 86 %). R_f = 0.4 (CH_2Cl_2/MeOH = 9:1). MS (ESI^+, MeOH) *m/z*: 651.2 $[M+H]^+$. The latter was considered pure enough, and batched for the next step. To a stirred solution of this Cbz-protected intermediate (60 mg, 0.092 mmol) in CH_2Cl_2/MeOH (5:5 mL), a NH_3 saturated methanolic solution (ca. 9 M, 10 mL) was added. After 5 min, cold water (10 mL) and then aq. NaOH (20% w/w, 1 mL) were added to the reaction mixture. The mixture was reduced *in vacuo* by 2/3 of its volume and acidified with aq HCl 2 M to pH = 5. The resulting mixture was stored overnight in the fridge at 0–4 °C and filtered. The solid was sequentially washed with H_2O (3 x 10 mL), petroleum ether (3 x 10 mL), and MeOH (1 x 10 mL) to provide the desired product **6** as a brown-yellow solid (30 mg, 63 %). $C_{26}H_{20}N_4O_6S$ (516.53). R_f = 0.28 (CH_2Cl_2/MeOH = 9:1). ^{1}H-NMR (400 MHz, DMF-d^7): δ 10.82 (s, 1H), 8.52 (s, 1H), 8.38 (s, 1H), 8.32 (d, *J* = 1.4 Hz, 1H), 8.23 (s, 1H), 8.19–8.13 (m, 2H), 7.87 (ddd, *J* = 8.6, 6.9, 1.7 Hz, 1H), 7.84–7.79 (m, 1H), 7.53 (ddd, *J* = 8.1, 6.8, 1.3 Hz, 1H), 6.71 (dd, *J* = 7.6, 6.0 Hz, 1H), 4.61 (td, *J* = 5.8, 2.9 Hz, 1H), 4.05 (q, *J* = 3.6 Hz, 1H),

3.81 (dd, J = 11.8, 4.0 Hz, 1H), 3.76 (dd, J = 11.9, 3.9 Hz, 1H), 2.67 (ddd, J = 13.3, 7.7, 5.7 Hz, 1H), 2.46 (ddd, J = 13.2, 6.1, 3.0 Hz, 1H). ^{13}C-NMR (101 MHz, DMF-d^7): δ 172.7, 155.1, 154.7, 148.4, 142.5, 138.2, 134.3, 134.1, 133.4, 130.5, 129.1, 125.2, 125.0, 122.5, 122.5, 118.6, 102.2, 97.2, 88.9, 87.5, 84.6, 81.4, 79.5, 71.8, 62.6, 41.2. MS (ESI$^+$, MeOH) *m/z*: 516.9 $[M+H]^+$. HRMS (ESI$^+$): *m/z* calcd for $C_{26}H_{21}N_4O_6S$: 517.1176 $[M+H]^+$; found 517.1190.

2.2.10. **2-(4-Bromothiophen-2-yl)-3-hydroxychromen-4-one (19):** To a stirred solution of **17** (883 μL, 7.345 mmol) and **18** (1.403 g, 7.345 mmol) in ethanol (15 mL), a 5 M NaOH solution (4.9 mL) was added dropwise. The reaction mixture was stirred 48 h at rt, before a dropwise addition of 30 % aq. hydrogen peroxide solution (2.1 mL). The resulting mixture was stirred for 30 min at rt, poured into cold water (75 mL) and then acidified with 2 M HCl to pH = 5. The resulting precipitate was filtered and thoroughly washed with water and cyclohexane to provide the desired product **19** as a yellow solid (500 mg, 21 %). $C_{13}H_7BrO_3S$ (323.16). R_f = 0.45 (toluene/EtOAc = 4:1). ^{1}H-NMR (400 MHz, DMSO-d^6): δ 10.63 (s, 1H), 8.10 (dd, J = 8.0, 1.6 Hz, 1H), 8.00 (d, J = 1.6 Hz, 1H), 7.90 (d, J = 1.5 Hz, 1H), 7.81 (ddd, J = 8.5, 6.8, 1.7 Hz, 1H), 7.78–7.73 (m, 1H), 7.47 (ddd, J = 8.1, 6.8, 1.3 Hz, 1H). ^{13}C-NMR (101 MHz, DMSO-d^6): δ 172.2, 154.2, 141.6, 137.5, 133.9, 133.9, 129.4, 128.2, 124.8, 124.7, 121.8, 118.2, 109.8. HRMS (ESI$^+$): *m/z* calcd for $C_{13}H_8BrO_3S$: 322.9372, 324.9352 $[M+H]^+$; found 322.9375, 324.9351.

2.2.11. **2-(4-Bromothiophen-2-yl)-3-(((benzyloxy)carbonyl)oxy)chromen-4-one (16):** To a stirred suspension of **19** (483 mg, 1.495 mmol) in CH_2Cl_2 (25 mL), 25% aq. KOH solution (5 mL), 18-crown-6 (7 mol%, 28 mg) and benzyl chloroformate (674 μL, 4.484 mmol, 3 eq) were added. The reaction mixture became homogenous after 2 h and was stirred overnight at rt. After quenching by addition of H_2O (40 mL), the organic layer was extracted with CH_2Cl_2 (3 x 30 mL), dried over $MgSO_4$, filtered and the volatiles were removed *in vacuo*. The residue was purified by flash chromatography on silica gel eluted with petroleum ether/EtOAc mixture (100:0 → 60:40, v/v) to provide the desired compound **16** as a light yellow solid (580 mg, 85 %). $C_{21}H_{13}BrO_5S$ (457.29). R_f = 0.4 (petroleum ether/AcOEt = 4:1). ^{1}H-NMR (400 MHz, CD_2Cl_2): δ 8.19 (dd, J = 8.0, 1.7 Hz, 1H), 7.84 (d, J = 1.5 Hz, 1H), 7.75 (ddd, J = 8.7, 7.1, 1.7 Hz, 1H), 7.63–7.53 (m, 2H), 7.51–7.34 (m, 6H), 5.35 (s, 2H). ^{13}C-NMR (101 MHz, CD_2Cl_2): δ 171.7, 155.6, 152.2, 150.5, 135.2, 134.9, 133.3, 132. 6, 129.7, 129.3, 129.2, 128.8, 126.2, 126.0, 124.1, 118.6, 111.9, 71.9. MS (ESI$^+$, MeOH) *m/z*: 457.0, 459.0 $[M+H]^+$. HRMS (ESI$^+$): *m/z* calcd for $C_{21}H_{14}BrO_5S$: 456.9740 $[M+H]^+$; found 456.9759.

3. Results and discussion

3.1. Preparation of the 3HC-based dA analogs

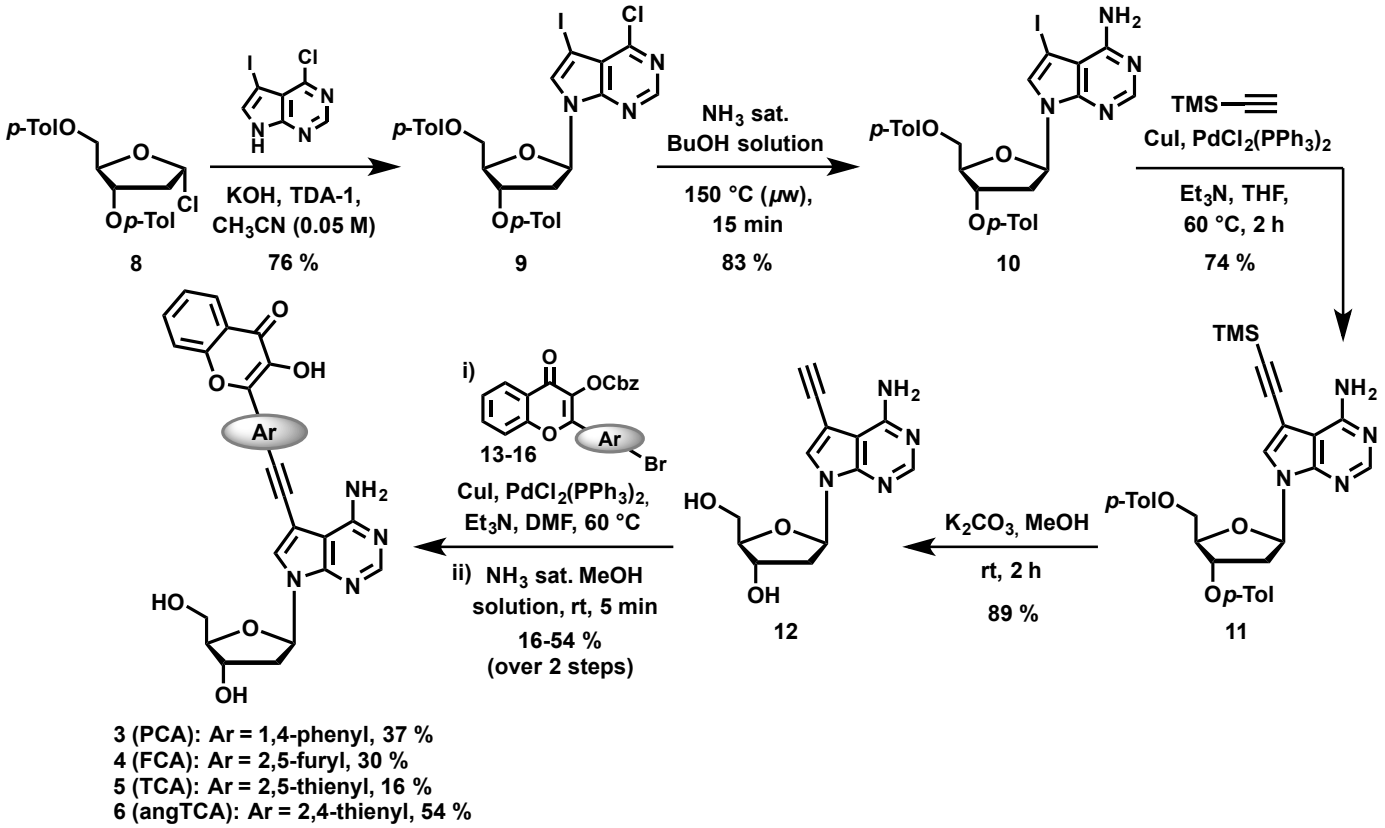

Scheme 2. Synthesis of the rationally designed dA analogs **3**–**6**, bearing a 3HC moiety as a fluorescent surrogate.

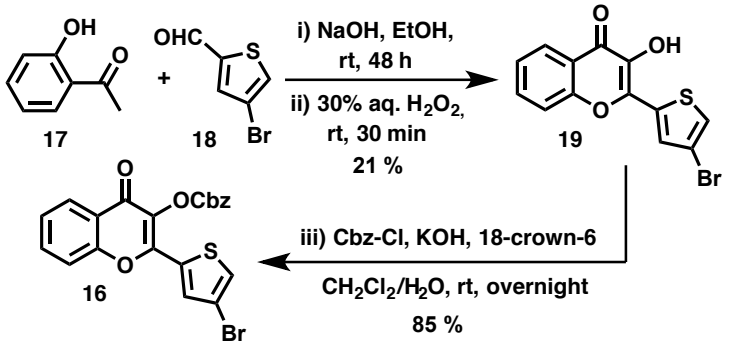

Scheme 3. Representative synthetic preparation of the Cbz-protected 3HC coupling partner **16**.

Like C5 of uracil, modifications at position 7 of adenine accommodate well into the hydrated major groove and minimally disturb base pairing and DNA structure. For that purpose, 7-deazaadenine is commonly used to attach of various reporting groups into DNA, including fluorescent ones [30,31,38,39]. Therefore, this scaffold was chosen to couple the 3HC fluorophore via an acetylenic moiety. A rigid and short linker was preferred in order to locate the dye in a precise position within the DNA major groove and to allow electronic communication between the nucleobase and the fluorophore. The targeted dA analogs, **3–6**, were synthesized according a convergent approach, involving a Sonogashira coupling between the 3HC fluorescent dye and 7-deaza-7-ethynyl-dA **12** as a key step (*Scheme 2*). The synthesis of intermediate **12** was directly inspired by Seela's previous work [37].

Nevertheless, we faced two critical challenges. First, for a reliable and scalable implementation, glycosylation of Hoffer's sugar **8** with 6-chloro-7-deaza-7-iodopurine must be conducted in diluted medium ([C] ≈ 0.05 M). The poor solubility of the nucleobase in acetonitrile makes the preparation of the anionic deazaadenyl moiety a limiting step. By taking this factor into account, the S_N2 type reaction provided the glycosylated product **9** in satisfying yields, and this key step was found to be scalable with reproducibility to the 1 g scale.

A second step for which we propose another solution concerns the amination of **9**. This S_NAr was performed initially under high-pressure in a stainless steel bomb. This approach also produced the unprotected nucleosides, which requires back protection of the free alcohols or working along the entire synthetic sequence with poorly soluble and polar compounds making the flash chromatography purifications more complex and low-yielding (*vide infra*). Microwave-assisted S_NAr amination has been used as an alternative to S_NAr amination [40]. The difficulty was to find suitable conditions, that offered the benefit of keeping *p*-toluoyl groups on the 3' and 5'-positions. We tried different conditions using microwave irradiation to meet this goal. To our delight, by screening the reaction time and temperature, but mostly by making use of *n*-BuOH as a solvent, we achieved complete chemoselectivity of S_NAr over the concomitant ester aminolysis affording **10** with good yields (83 %)‡. Introduction of the short and rigid alkynyl linker was achieved in two steps through a conventional Sonogashira coupling in the presence of TMS-acetylene followed by a methanolysis leading to **12** with satisfactory yields. This ethynyl derivative **12** constitutes the essential building block for the final assembly of the targeted two-colors dA analogs **3–6**.

In parallel, the protected 3HC-coupling partner was prepared by a one-pot, two-step procedure, involving a Claisen-Schmidt condensation of *o*-hydroxyacetophenone on a (hetero)aromatic aldehyde through an alkaline treatment followed by an Algar-Flynn-Oyamada reaction. This oxidative cyclization concomitantly occurs by addition of hydrogen peroxide to the basic media [41]. The reactive 3-OH was then masked by the Cbz group following a known procedure [42]. Compounds **13–15** were synthesized as previously reported [13,28]. Representative synthetic access was depicted in *Scheme 3* for the 2-(4-bromothienyl)-3HC derivative **16** required to obtain **angTCA 6**. With the 2 coupling partners in hand, their electronic conjugation was efficiently carried out using classical Sonogashira reaction conditions. Carbonate aminolysis was conducted under methanolic ammonia treatment to provide **PCA**, **FCA**, **TCA**, and **angTCA 3–6**. Although removal of the protecting group proceeded cleanly, the poor solubility of final naked nucleosides made their purification difficult.

As for r**evTCA 7**, the reversed orientation of the dipole moment necessitates an adaptation of the retrosynthetic access. In this approach, the ethynyl connector was first introduced to the 3HC before the assembly with the 7-deaza-7-iodo adenylate derivative **10**. The corresponding synthesis is described in SI (*Schemes S1&S2*). Methanolysis yielded **revTCA 7**, the last dA analog of this study with an inverted D-π-A design (D= thienyl, A= carbonyl group).

3.2. Photophysical characterization

3.2.1. Comparison with parent 3HCs

Absorption and emission properties of **TCA**, **FCA**, **PCA**, **angTCA** and **revTCA**, were first characterized in MeOH. To evaluate the impact on the photophysics of the aromatic linker conjugating 7-ethynyl-dA with 3HC, these data were compared to those of the parent 2-phenyl-, 2-furyl-, and 2-thienyl-3HCs, respectively **PC**, **FC,** and **TC** from which they originate (*Table 1*).

All conjugates exhibited a dual emission in MeOH, with the short and long wavelength bands that can be assigned to the N* and T* states, but with different features. Compared to their parent compounds, **PCA**, **FCA** and **TCA**, but not **angTCA** and **revTCA**, displayed significant red-shifted absorption and emission maxima that resulted in substantial improvements of their spectroscopic properties. Thus, the five compounds can be classified into two sets of dyes.

Table 1. Spectroscopic comparison in MeOH of parent 2-aryl-3HCs (**PC**, **FC** and **TC**) and their corresponding dA conjugates (**PCA**, **FCA**, **TCA**, **angTCA**, and **revTCA**).[a]

	ε_{max} [b]	λ_{Abs} [c]	λ_{N^*} [d]	$\Delta\lambda_{N^*}$ [f]	λ_{T^*} [e]	I_{N^*}/I_{T^*} [g]
PC	18	343	401	–	532	0.24
PCA	30	364	464	63	551	0.31
FC	22	356	418	–	532	0.86
FCA	33	383	484	66	561	0.69
TC	21	359	423	–	542	0.41
TCA	31	392	492	69	569	0.48
angTCA	18	361	425	2	543	0.05
revTCA	21	356	429	6	551	0.16

[a] Reported values are the average of two or more independent and reproducible measurements, ±1 nm for wavelengths. Excitation wavelength was at the corresponding absorption maximum. [b] Molar absorptivity in 10^3 $M^{-1}\cdot cm^{-1}$. [c] Position of the absorption maximum in nm. [d,e] Positions of the normal N* and T* band maxima in nm, respectively. [f] Difference of emission N* maxima between the conjugate and the parent 3HC in nm. [g] Ratio intensity of the two emission maxima.

Upon conjugation of 7-ethynyl-dA with **PC**, **FC**, and **TC**, the resulting two-color nucleosides **PCA**, **FCA**, and **TCA** displayed: *i)* a 1.5-fold increase of their molar absorptivity, *ii)* a 20–35 nm bathochromic shift of their absorption and tautomer T* maxima, as well as *iii)* a significant redshift of their N* maxima (60–70 nm). *Figure 3* shows **TCA** *vs.* **TC** as a representative example. The shift of absorption and emission maxima to longer wavelengths follows the same sequence as for the parent dyes: **PCA** < **FCA** < **TCA** (*Figure 4*). These observations are in line with previous studies and can be attributed to the fact that the 2-furyl- and 2-thienyl rings allow a more planar conformation for conjugation in comparison to the 2-phenyl ring [43]. Thus, the conjugation of furyl- and thienyl-3HC with 7-deazaadenine resulted in the strongest improvement of their spectroscopic properties. By contrast, **angTCA** and **revTCA** exhibited absorption and emission properties comparable to that of the parent **TC** dye (*Figure 4*). The increased absorptivity and the bathochromic shifts of

absorption and emission are observed when dA and chromone are coupled using the 1,4-phenyl (**PCA**), 2,5-furyl (**FCA**) and 2,5-thienyl (**TCA**) central connectors. These aromatic linkers, but not the 2,4- and reverse thienyl-3HC, allow mesomeric coupling between the electron-donating enamino nitrogen *N9* of 7-deazadadenine and the electron-withdrawing carbonyl of 3HC. The photophysics observed for these connectors support the hypothesis of an established push–pull relationship between the nucleobase and the original fluorophore. All these observations are consistent with those reported previously for the uracil series [13].

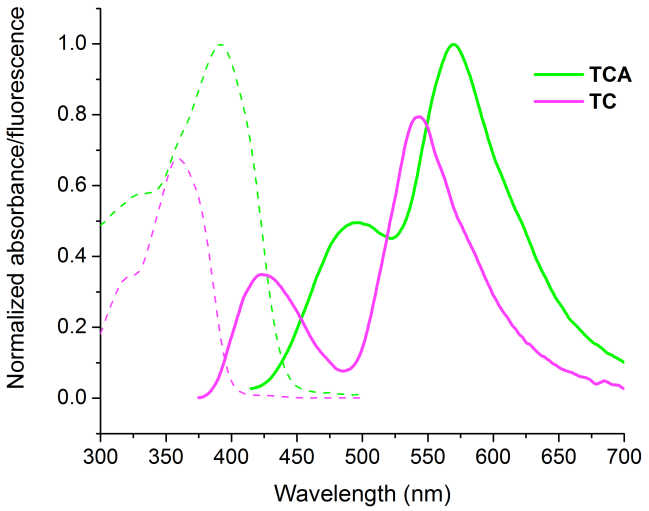

Figure 3. Absorption (*dashed lines*) and fluorescence (*solid*) emission spectra of **TC** (magenta), and **TCA** (green) in MeOH. *Excitation wavelength corresponds to the absorbance maximum of each compound. Absorptions and emissions are proportional to their absorptivity and quantum yield, respectively.*

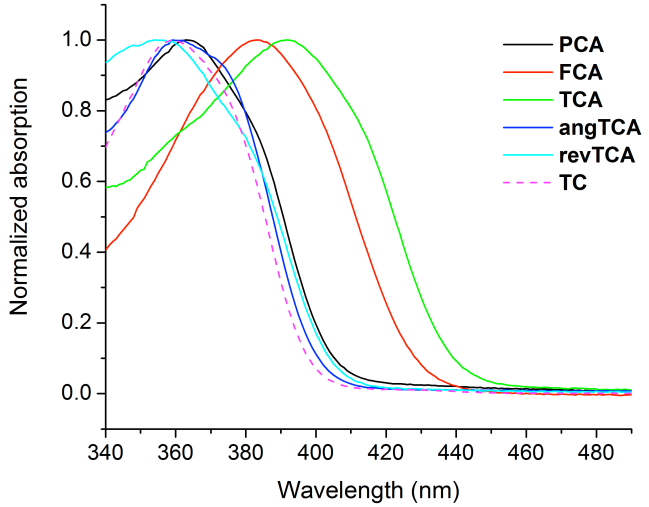

Figure 4. Normalized absorption spectra in MeOH of the five 3HC-based dA analogs (*solid lines*) and the parent chromone **TC** (*dashed*).

*3.2.2. Comparison between **FCA** and **TCA***

The most prospective **FCA** and **TCA** dyes were subsequently studied in a set of solvents with a wide range of polarities to provide further insight into their photophysical properties. Three protic (MeOH, EtOH and *i*-PrOH) and seven aprotic solvents (CH_3CN, DMSO, Acetone, EtOAc, THF, Dioxane and Toluene) were investigated. The solvent polarity was ranked using the Dimroth-Reichardt $E_T^N(30)$ scale [44]. This empirical scale takes into account the dielectric constant and H-bond donating ability of the solvent. It is normalized from TMS (0) to water (1). The empirical Abraham $\Sigma\beta_2^H$ parameter was selected to rank the H-bonding basicity of the solvent (*Table 2*)[45].

FCA and **TCA** showed a single band absorption centered at 381−391 and 389–400 nm, respectively (*Figures S2*). The absorption spectra of these dyes are almost independent of solvent polarity demonstrating little solvatochromism. By contrast, the dyes showed dual emissions in all tested solvents with strong sensitivity to the polarity changes (*Figures 5 & S3*). Superimposition of the absorption curves with the excitation spectra from N* and T* bands confirmed that dual-emissive signature originates from an ESIPT process (*Figure S4*).

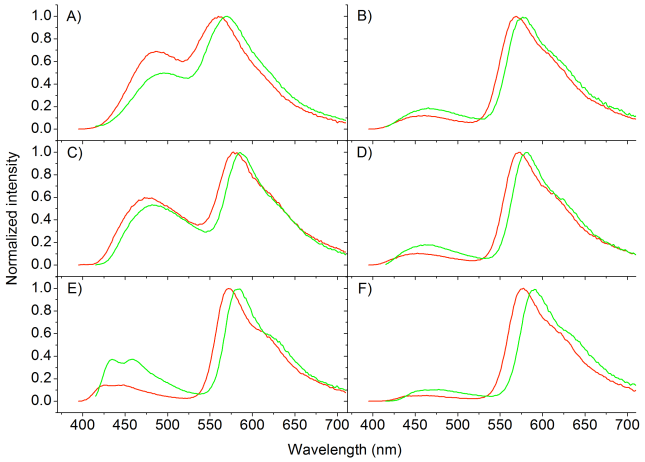

Figure 5. Fluorescence spectra of **FCA** (red) and **TCA** (green) in different organic solvents: A) MeOH, B) acetonitrile, C) DMSO, D) acetone, E) dioxane, and F) toluene.

From toluene to methanol, the N* bands of **FCA** and **TCA** shifted to the red by 41 and 37 nm, respectively (*Figure S5*); while for the parent **TC**, the shift was halved (18 nm, *Figure S6*). The positive solvatochromism of the N* is typical of dyes with ICT character [46]. To estimate their ICT ability, the polarity scale of Lippert-Mataga was used (*Table S1*, *Figures S9 & S10*)[47]. Plotting the Stokes shifts for aprotic solvents as a function of the orientation polarizability showed linear fits with positive slopes for the compounds (*Figure S10*). Extracting the slopes allowed us to calculate the difference in dipole moments between the excited and ground states for **FCA** and **TCA** (7.0 and 7.1 D, respectively). A 3-fold increase of the dipole moment difference was observed when **TCA** was compared with **TC** (7 *vs.* 2.3 D, respectively). These results are consistent with a larger increase of dipole moments of the normal excited states for **FCA** and **TCA** after light absorption, further supporting a push–pull D-π-A connectivity between the nucleobase and the 3HC moiety (blue to red atoms, *Figure 2*).

The positions of T* band maxima of **FCA** and **TCA** were shifted to the blue in protic solvents, as compared with aprotic ones, likely as a consequence of the formation of a H bond between the chromone phenoxide in the excited tautomer and the alcohols, as was proposed for **FC** [48]. The Stokes shifts for the first and second emission bands of **FCA** and **TCA** are comprised between 56–101 and 177–193 nm, respectively. The large Stokes shifts obtained for the lowest energy emission bands are typical of ESIPT dyes. As a general trend, the I_{N*}/I_{T*} ratio increased along with solvent polarity (*Figures 5 & S3*). The highest I_{N*}/I_{T*} ratios were observed for both strongly polar methanol (protic) and DMSO (aprotic), whereas the lowest values were noted for the most apolar toluene (*Table 2*). It is noteworthy that H-bonding dominates the polarity effect as evidenced by analyzing the plots of I_{N*}/I_{T*} ratio *vs.* $E_T^N(30)$. For instance, *Figure 6* illustrates the linear fits obtained for **FCA** in aprotic and protic solvents (for **TCA**, *Figure S7*). For protic solvents, the slopes were steeper, highlighting superior sensitivity of the dyes to the probe's protogenic medium. These results also indicate specific interactions between the solvent and the dye. These properties are classical features of 3HC probes [49,50].

Table 2. Photophysical properties of **FCA**, **TCA**, **angTCA** and **revTCA** in different solvents.[a]

		ε_{max} (10^3 M^{-1}·cm^{-1})[b]	33	31	18	21	21
Solvent	$E_T^N(30)$[c]	$\Sigma\beta_2^H$[d]	λ (nm), Φ (%)[e,f]	**FCA**	**TCA**	**angTCA**	**revTCA**	**TC**
MeOH	0.76	0.47	λ_{Abs}	383	392	361	356	359
			λ_{N*}	484	492	425	429	423
			λ_{T*}	561	569	543	551	542
			I_{N*}/I_{T*}	0.69	0.48	0.05	0.16	0.41
			Φ	4	5	0.5	2	4
EtOH	0.65	0.48	λ_{Abs}	384	393	360	356	360
			λ_{N*}	479	487	421	425	420
			λ_{T*}	566	574	547	555	545
			I_{N*}/I_{T*}	0.31	0.22	0.04	0.09	0.18
			Φ	12	11	1	3	6
i-PrOH	0.57	0.48	λ_{Abs}	387	394	362	358	361
			λ_{N*}	478	483	418	422	417
			λ_{T*}	566	575	547	554	544
			I_{N*}/I_{T*}	0.20	0.15	0.03	0.07	0.11
			Φ	23	22	4	4	7
CH_3CN	0.46	0.32	λ_{Abs}	381	389	355	353	354
			λ_{N*}	459	465	421	419	409
			λ_{T*}	570	576	544	549	543
			I_{N*}/I_{T*}	0.13	0.18	0.01	0.04	0.03
			Φ	18	16	1	1	7
DMSO	0.44	0.88	λ_{Abs}	391	400	364	359	361
			λ_{N*}	478	482	428	432	422
			λ_{T*}	579	587	552	557	549
			I_{N*}/I_{T*}	0.65	0.55	0.09	0.06	0.05
			Φ	21	19	0.5	2	8
Acetone	0.35	0.49	λ_{Abs}	382	390	356	354	354
			λ_{N*}	456	463	418	416	408
			λ_{T*}	572	582	548	555	547
			I_{N*}/I_{T*}	0.11	0.19	0.02	0.08	0.04
			Φ	18	24	3	2	7
EtOAc	0.23	0.45	λ_{Abs}	382	392	356	354	354
			λ_{N*}	447	460	412	413	406
			λ_{T*}	571	582	547	553	545
			I_{N*}/I_{T*}	0.07	0.14	0.02	0.03	0.02
			Φ	22	25	20	10	13
THF	0.21	0.48	λ_{Abs}	385	394	359	356	356
			λ_{N*}	447	459	411	411	406
			λ_{T*}	575	586	550	556	549
			I_{N*}/I_{T*}	0.10	0.21	0.03	0.07	0.06
			Φ	28	32	24	14	18
Dioxane	0.16	0.64	λ_{Abs}	385	394	359	356	356
			λ_{N*}	443	455	409	410	405
			λ_{T*}	572	583	548	556	547
			I_{N*}/I_{T*}	0.15	0.37	0.04	0.06	0.04
			Φ	25	26	25	19	18
Toluene	0.10	0.14	λ_{Abs}	387	396	362	358	357
			λ_{N*}	443	455	408	410	406
			λ_{T*}	577	589	551	558	548
			I_{N*}/I_{T*}	0.04	0.1	0.02	0.02	0.01
			Φ	33	27	39	31	33

[a] Similar to *Table 1*. [b] Molar extinction coefficient was determined in methanol; relative standard deviations are lower or equal to 5 %. [c] Reichardt's empirical solvent polarity index [44]. [d] H-bond basicity [45]. [e] Position of the absorption maximum in nm; maximum of the normal N* emission band in nm; maximum of the tautomer T* emission in nm; ratio of the intensities at the two emission maxima. [f] Fluorescence quantum yields Φ were determined using an excitation at the corresponding absorption maximum of each compound in the considered solvent. Quinine sulfate in 0.5 M H_2SO_4 solution (λ_{Ex} = 350 nm, Φ = 55 %)[51] and *p*-DiMethylAminoFlavone (DMAF) in EtOH (λ_{Ex} = 404 nm, Φ = 27 %)[52] were used as standard references, ±10 % mean standard deviation.

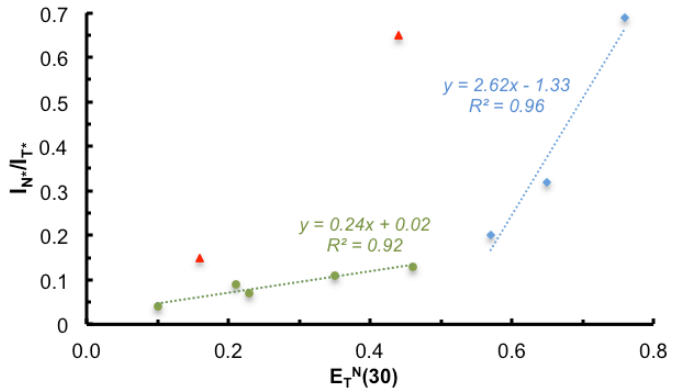

Figure 6. Intensity ratio I_{N^*}/I_{T^*} of **FCA** as a function of the normalized Reichardt's parameter $E_T^N(30)$. *The green circles and blue diamonds represent aprotic (toluene, dioxane, THF, EtOAc, acetone, CH_3CN) and protic (MeOH, EtOH, i-PrOH) solvents, respectively. The green and blue dashed lines represent the corresponding linear fitting curves. The red triangles represent the results of DMSO and dioxane.*

Specific interactions were also noticed for **FCA** and **TCA** in DMSO, and to a lower extent in dioxane, as those solvents showed upward deviations from the linear fits of aprotic solvents (*Figures 6 & S7*). These deviations were evidenced only for the two most basic aprotic solvents (*Table 2*, $\Sigma\beta_2^H$ = 0.88 and 0.68), with the most basic DMSO displaying the most pronounced effect. These deviations indicate that basic solvents frustrate the ESIPT reaction in **FCA** and **TCA**, likely by disrupting the intramolecular H-bonding. There are precedents in the literature of 3HCs, where the basicity of the solvent has an important influence on the variation of the intensity ratio [53,54]. Similar behavior was also observed for 3-hydroxyquinolones [55,56].

Thus, the superior absorptivity of **FCA** and **TCA** (1.5 fold, *Table 1*) together with their solvatochromic properties compares them favorably with the parent **FC** and **TC** dyes.

Since both **FCA** and **TCA** have similar molar absorptivity (~30,000, *Table 1*) comparing the quantum yields will directly give information on the brightness of the dual emitters. From a general point of view, QYs were rather good in all tested solvents except MeOH and EtOH, oscillating between 16–33 %. In EtOH and MeOH, the quantum yields drop to 11–12 and 4–5%, respectively. This behavior is common in strong polar solvents like MeOH for dyes exhibiting a significant ICT character. Considering the strong donating ability of the *N*9 enamine, angular and reversed assemblies were thus considered (**angTCA** and **revTCA**), to reduce quenching in a polar protogenic medium by weakening the excited-state dipole moment (*Figure 2*).

*3.2.3. Breaking the N9 conjugation: **angTCA** and **revTCA***

In all solvents, the absorption maxima of **angTCA** and **revTCA** were centered around 360 nm as for **TC** (*Table 2 & Figures 4 & S2*). Both dyes also displayed similar absorptivity close to that of **TC** (*Table 1*). The absorption properties of **angTCA** and **revTCA** are consistent with an electronic disconnection between 7-ethynyl-dA and **TC**.

Concerning the fluorescence features, the two emission maxima appeared close to those of the parent chromone **TC**. Depending on the solvent polarity, N* and T* fluctuated between 408–432 and 543–558 nm, respectively (*Figure S6*). The weak solvatochromism on the N* emission band demonstrated the attenuated push–pull relationship relating the thienyl and the carbonyl in line with the low dipole moment differences calculated for **angTCA** and **revTCA** as for **TC** (compare 3.8 and 2.8 D with 2.3 D, *Table S1 & Figure 2*).

3.2.4. Behavior in a protogenic environment and PET

The main differences in photophysics that can be raised between both **angTCA** and **revTCA** conjugates and **TC** are the sensitivity for ratiometric sensing of the protic environment and the brightness in polar media. Indeed, **TC** is known to be one of the most sensitive 2-aryl-3HCs to probe H-bond donating solvents [13]. For instance, comparing the intensity ratios along the increasing proticity (*i*-PrOH, EtOH and MeOH) **angTCA** revealed to be almost insensitive (0.03 → 0.04 → 0.05), whereas **revTCA** showed a moderate increment of its N* emission band (0.07 → 0.09 → 0.16), in comparison to the parent **TC** (0.11 → 0.18 → 0.41). Moreover, both conjugates demonstrated more pronounced quenching than **TC** with the growing proticity of solvents. One plausible explanation to account for these observations in protic medium is a Photoinduced Electron Transfer (PET) from the 7-deazaadenine moiety to the 3HC [57].

PET is the photoquenching process by which an excited electron is transferred from a donor to an acceptor. This excited-state redox reaction is one form of photoquenching [47]. During our previous work on ODN labeling, fluorescence quenching of 3HC by flanking or opposite G was regularly observed. Among the 4 nucleobases, G is known to be the most reductive one because it has the lowest redox potential [58,59]. 7-deazaadenine possesses a similar feature [60]. Hence, in a polar protogenic solvent, the PET process is highly favored, likely through a proton-coupled process [61-64]. To prove this phenomenon, the idea was to protonate the nucleobase (*Figure 7*), which should raise the redox potential of the 7-deazaadenine moiety and inhibit the coupled proton and electron transfer. To test this hypothesis, TFA (1 ‰, v/v) was added to a methanolic solution of each dye while monitoring the fluorescence emission.

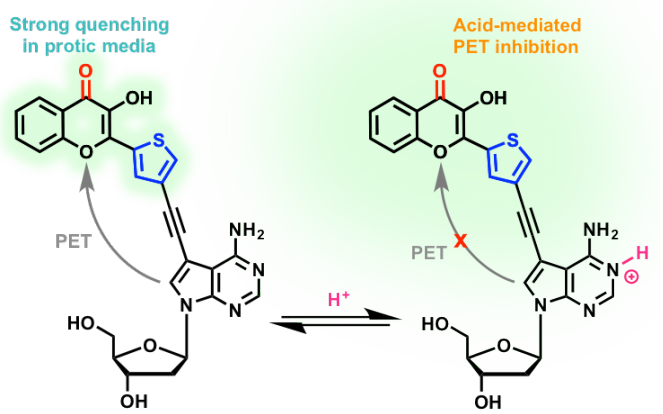

Figure 7. Schematic representation of the proposed acid-mediated PET inhibition.

As depicted on *Figure 8*, addition of TFA supports this interpretation. The dual emission of each dye was turned on, reaching a 2- and 29-fold increase of the fluorescence intensity for **revTCA** and **angTCA**, respectively (*Figures 8 & S8*). Similar treatment of **TC** showed no difference. Interestingly, when **PCA**, **FCA**, and **TCA** were treated in MeOH by adding TFA, the emission intensity was multiplied from 5 to 15 (*Figures 8 & S8*). These results suggest that PET is a plausible quenching mechanism for all the new conjugates.

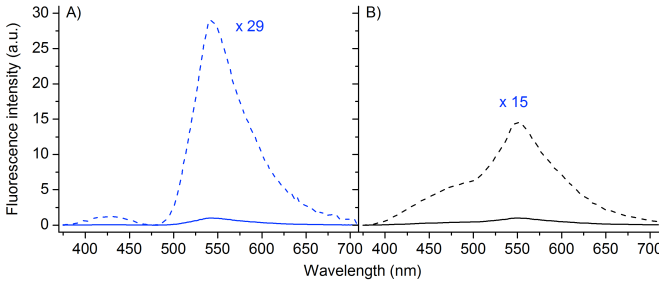

Figure 8. Turn-on emission in MeOH upon TFA addition for A) **angTCA** (*blue*) B) **PCA** (*black*) as representative examples of the acid-mediated PET inhibition.

Since **TCA** and **FCA** aim to be incorporated in DNA, similar experiments were conducted in water. Addition of TFA resulted in an impressive fluorescence turn-on leading to 8- and 14-fold enhancements of the signal respectively (*Figure 9*).

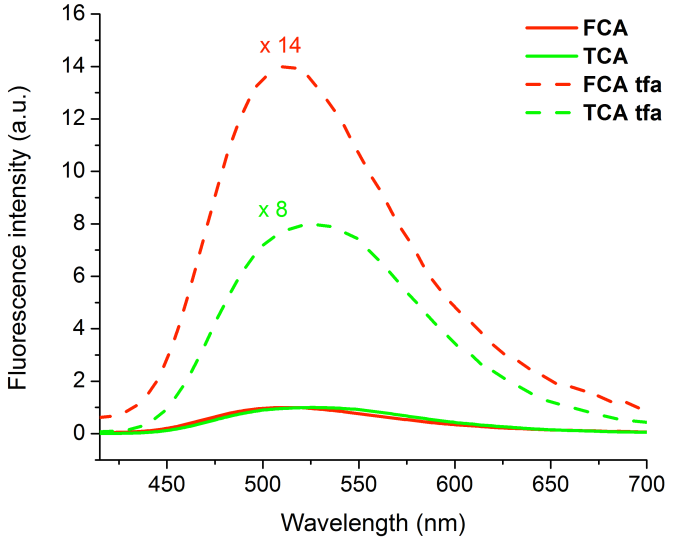

Figure 9. Fluorescence turn-on in water upon TFA addition for **FCA** (red) and **TCA** (green).

These observations open up new prospects to utilize this acid-mediated PET inhibition for sensing the folding of adenine (A)-rich DNA sequences. The A-motif, also called poly(A) exhibits a unique secondary structure at acidic pH based on a right-handed helical duplex with parallel-mannered chains and tilted protonated A^+ bases [65].

4. Conclusion

To summarize, 5 dual-emissive dA nucleoside analogs incorporating 7-deazaadenine as a base and a 2-aryl-3HC as an initial fluorophore, were rationally designed and synthesized by a convergent and scalable approach. Their photophysics were investigated in solvents of various polarities to determine their ability to detect subtle environmental changes. During these spectroscopic investigations, a PET process appears to have occurred between the electron-rich nucleobase and the two-color dye, resulting in a strongly quenched fluorescence signal in a protogenic medium. Protonation of the nucleobase was found to resuscitate a well-resolved dual emission through a dramatic turn-on mechanism. The fully conjugated **FCA** and **TCA** were revealed to be the most promising emitters in terms of photophysical features including: *i)* a visible absorption allowing a violet excitation, *ii)* a two-channel fluorescence signature with strong N* positive solvatochromism and significant T* hypsochromic shift, *iii)* a ratiometric response that is highly sensitive to H-bonding and solvent basicity, and *iv)* a brightness exacerbated at lower pH. Hence, both multiparametric dyes present appealing characteristics for the sensing of acid-mediated A-motif folding. This is the current focus of our ongoing research and will be reported in due time.

Acknowledgments

We thank for the PhD grants of H.-N.L and G.B., the ANR (UCAJEDI project: ANR-15-IDEX-01) and the French Government, respectively; and for the postdoctoral fellowship of C.Z, the PACA region (DNAfix-2014-07199). This research was financially supported by the ANR (ANR-12-BS08-0003-02) and PACA region (DNAfix-2014-02862).

Supplementary Material

Supplementary material, including synthetic protocols and characterization (NMR, absorption, fluorescence) of products, is provided as a separate electronic PDF file and is available free of charge on the ELSEVIER website at DOI: xxxxxxxxxxxxxxxxxx

References and notes

‡ The only limitation to the scale-up of this reaction is the reception capacity of the heating area in the microwave apparatus with a fixed concentration.

[1] Herdewijn P, Ed. Modified Nucleosides: in Biochemistry, Biotechnology and Medicine; Wiley-VCH: Weinheim, Germany, 2008, pp. 1−658.

[2] Nakatani K, Tor Y, Eds. Modified Nucleic Acids, Nucleic Acids and Molecular Biology Series (31); Springer International Publishing AG: Cham, Switzerland, 2016, pp. 1–276.

[3] Wilhelmsson LM, Tor, Y, Eds. Fluorescent Analogues of Biomolecular Building Blocks: Design and Applications; John Wiley & Sons Inc.: Hoboken, NJ, 2016, pp. 1−448.

[4] Xu W, Chan KM, Kool ET. Fluorescent nucleobases as tools for studying DNA and RNA. Nature Chem 2017;9:1043–55. doi:10.1038/NCHEM.2859.

[5] Daniels M, Hauswirth W. Fluorescence of the purine and pyrimidine bases of the nucleic acids in neutral aqueous solution at 300 degrees K. Science 1971;171:675–7.

[6] Pecourt JML, Peon J, Kohler B. Ultrafast internal conversion of electronically excited RNA and DNA nucleosides in water. J Am Chem Soc 2000;122:9348–9. doi:10.1021/ja0021520.

[7] Nir E, Kleinermanns K, Grace L, de Vries MS. On the Photochemistry of Purine Nucleobases. J Phys Chem A 2001;105:5106–10. doi:10.1021/jp0030645.

[8] Onidas D, Markovitsi D, Marguet S, Sharonov A, Gustavsson T. Fluorescence properties of DNA nucleosides and nucleotides: A refined steady-state and femtosecond investigation. Journal of Physical Chemistry B 2002;106:11367–74. doi:10.1021/jp026063g.

[9] Sinkeldam RW, Greco NJ, Tor Y. Fluorescent Analogs of Biomolecular Building Blocks: Design, Properties, and Applications. Chem Rev 2010;110:2579–619. doi:10.1021/cr900301e.

[10] Wilhelmsson LM. Fluorescent nucleic acid base analogues. Q Rev Biophys 2010;43:159–83. doi:10.1017/S0033583510000090.

[11] Demchenko AP. Optimization of fluorescence response in the design of molecular biosensors. Anal

Biochem 2005;343:1–22. doi:10.1016/j.ab.2004.11.041.

[12] Demchenko AP. Introduction to Fluorescence Sensing, 2nd ed.; Springer Netherlands: Heidelberg, Germany, 2015, pp. 1–794.

[13] Barthes NPF, Karpenko IA, Dziuba D, Spadafora M, Auffret J, Demchenko AP, et al. Development of environmentally sensitive fluorescent and dual emissive deoxyuridine analogues. RSC Adv 2015;5:33536–45. doi:10.1039/C5RA02709H.

[14] Zhao J, Ji S, Chen Y, Guo H, Yang P. Excited state intramolecular proton transfer (ESIPT): from principal photophysics to the development of new chromophores and applications in fluorescent molecular probes and luminescent materials. Phys Chem Chem Phys 2012;14:8803–17. doi:10.1039/C2CP23144A.

[15] Sedgwick AC, Wu L, Han H-H, Bull SD, He X-P, James TD, et al. Excited-state intramolecular proton-transfer (ESIPT) based fluorescence sensors and imaging agents. Chem Soc Rev 2018;46:7105–39. doi:10.1039/C8CS00185E.

[16] Jacquemin D, Khelladi M, De Nicola A, Ulrich G. Turning ESIPT-Based triazine fluorophores into dual emitters_ From theory to experiment. Dyes Pigm 2019;163:475–82. doi:10.1016/j.dyepig.2018.12.023.

[17] Serdiuk IE, Roshal AD. Exploring double proton transfer: A review on photochemical features of compounds with two proton-transfer sites. Dyes Pigm 2017;138:223–44. doi:10.1016/j.dyepig.2016.11.028.

[18] Demchenko AP, Klymchenko AS, Pivovarenko VG, Ercelen S. Ratiometric Probes: Design and Applications. In Kraayenhof R, Visser AJWG, Gerritsen HC, Eds.: *Fluorescence spectroscopy, imaging and probes: new tools in chemical physical and life sciences*, Springer series on fluorescence, Vol. 2; Springer-Verlag Berlin Heidelberg, 2002, pp. 101–10.

[19] Demchenko AP. The concept of λ-ratiometry in fluorescence sensing and imaging. J Fluoresc 2010;20:1099–128. doi:10.1007/s10895-010-0644-y.

[20] Klymchenko AS, Mély Y. Fluorescent Environment-Sensitive Dyes as Reporters of Biomolecular Interactions. In Morris MC, Ed.: *Progress in Molecular Biology and Translational Science*, Vol. 113; Academic Press: Burlington, MA, 2013, pp. 35–58.

[21] Demchenko AP. Practical aspects of wavelength ratiometry in the studies of intermolecular interactions. J Mol Struct 2014;1077:51–67. doi:10.1016/j.molstruc.2013.11.045.

[22] Spadafora M, Postupalenko VY, Shvadchak VV, Klymchenko AS, Mély Y, Burger A, et al. Efficient Synthesis of Ratiometric Fluorescent Nucleosides Featuring 3-Hydroxychromone Nucleobases. Tetrahedron 2009;65:7809–16. doi:10.1016/j.tet.2009.07.021.

[23] Dziuba D, Postupalenko VY, Spadafora M, Klymchenko AS, Guérineau V, Mély Y, et al. A Universal Nucleoside with Strong Two-Band Switchable Fluorescence and Sensitivity to the Environment for Investigating DNA Interactions. J Am Chem Soc 2012;134:10209–13. doi:10.1021/ja3030388.

[24] Kuznetsova AA, Kuznetsov NA, Vorobjev YN, Barthes NPF, Michel BY, Burger A, et al. New environment-sensitive multichannel DNA fluorescent label for investigation of the protein-DNA interactions. PLoS One 2014;9:e100007. doi:10.1371/journal.pone.0100007.

[25] Kilin V, Gavvala K, Barthes NPF, Michel BY, Shin D, Boudier C, et al. Dynamics of Methylated Cytosine Flipping by UHRF1. J Am Chem Soc 2017;139:2520–8. doi:10.1021/jacs.7b00154.

[26] Sholokh M, Sharma R, Grytsyk N, Zaghzi L, Postupalenko VY, Dziuba D, et al. Environmentally Sensitive Fluorescent Nucleoside Analogues for Surveying Dynamic Interconversions of Nucleic Acid Structures. Chem - Eur J 2018;5:388–13. doi:10.1002/chem.201802297.

[27] Zargarian L, Ben Imeddourene A, Gavvala K, Barthes NPF, Michel BY, Kenfack CA, et al. Structural and Dynamical Impact of a Universal Fluorescent Nucleoside Analogue Inserted Into a DNA Duplex. J Phys Chem B 2017;121:11249–61. doi:10.1021/acs.jpcb.7b08825.

[28] Dziuba D, Karpenko IA, Barthes NPF, Michel BY, Klymchenko AS, Benhida R, et al. Rational design of a solvatochromic fluorescent uracil analogue with a dual-band ratiometric response based on 3-hydroxychromone. Chem - Eur J 2014;20:1998–2009. doi:10.1002/chem.201303399.

[29] Barthes NPF, Gavvala K, Dziuba D, Bonhomme D, Karpenko IA, Dabert-Gay AS, et al. Dual emissive analogue of deoxyuridine as a sensitive hydration-reporting probe for discriminating mismatched from matched DNA and DNA/DNA from DNA/RNA duplexes. J Mater Chem C 2016;4:3010–7. doi:10.1039/C5TC03427B.

[30] Saito Y, Suzuki A, Ishioroshi S, Saito I. Synthesis and photophysical properties of novel push–pull-type solvatochromic 7-deaza-2′-deoxypurine nucleosides. Tetrahedron Lett 2011;52:4726–9. doi:10.1016/j.tetlet.2011.06.089.

[31] Suzuki A, Kimura K, Ishioroshi S, Saito I, Nemoto N, Saito Y. Synthesis of solvatofluorochromic 7-arylethynylated 7-deaza-2′-deoxyadenosine derivatives: application to the design of environmentally sensitive fluorescent probes forming stable DNA duplexes. Tetrahedron Lett 2013;54:2348–52. doi:10.1016/j.tetlet.2013.02.063.

[32] Armarego WLF, Ed. Purification of laboratory chemicals, 8th ed.; Elsevier Butterworth-Heinemann: Oxford, 2017, pp. 1–1198.

[33] Jork H, Funk W, Fischer WR, Wimmer H, Eds. Thin-Layer Chromatography: Reagents and Detection Methods, Vol. 1a, Physical and Chemical Detection Methods: Fundamentals, Reagents I; VCH: Weinheim, Germany, 1990, pp. 1–464.

[34] Still WC, Kahn M, Mitra A. Rapid chromatographic technique for preparative separations with moderate resolution. J Org Chem 1978;43:2923–5. doi:10.1021/jo00408a041.

[35] Gottlieb HE, Kotlyar V, Nudelman A. NMR Chemical Shifts of Common Laboratory Solvents as Trace Impurities. J Org Chem 1997;62:7512–5.

[36] Fulmer GR, Miller AJM, Sherden NH, Gottlieb HE, Nudelman A, Stoltz BM, et al. NMR Chemical Shifts of Trace Impurities: Common Laboratory Solvents, Organics, and Gases in Deuterated Solvents Relevant to the Organometallic Chemist. Organometallics 2010;29:2176–9. doi:10.1021/om100106e.

[37] Seela F, Zulauf M. Palladium-catalyzed cross coupling of 7-iodo-2'-deoxytubercidin with terminal alkynes. Synthesis 1996:726–30.
[38] Suzuki A, Nemoto N, Saito I, Saito Y. Design of an environmentally sensitive fluorescent 8-aza-7-deaza-2′-deoxyadenosine derivative with dual fluorescence for the specific detection of thymine. Org Biomol Chem 2014;12:660–6. doi:10.1039/C3OB41757C.
[39] Saito Y, Suzuki A, Yamauchi T, Saito I. Design and synthesis of 7-naphthyl-8-aza-7-deaza-2′-deoxyadenosines as environmentally sensitive fluorescent nucleosides. Tetrahedron Lett 2015;56:3034–8. doi:10.1016/j.tetlet.2014.10.116.
[40] Bazureau J-P, Paquin L, Carrié D, L'Helgoual'ch J-M, Guihéneuf S, Wacothon K, et al. Microwaves in Heterocyclic Chemistry. In de la Hoz A, Loupy A, Eds.: *Microwaves in Organic Synthesis, 3rd ed., Part II: Applications of Microwave Irradiation*; Wiley-VCH: Weinheim, Germany, 2013, pp. 673−735.
[41] Dean FM, Podimuang V. 737. The course of the Algar–Flynn–Oyamada (A.F.O.) reaction. J Chem Soc Perkin Trans 1965;0:3978–87. doi:10.1039/JR9650003978.
[42] Dziuba D, Benhida R, Burger A. A Mild and Efficient Protocol for the Protection of 3-Hydroxychromones Under Phase-Transfer Catalysis. Synthesis 2011:2159–64.
[43] Klymchenko AS, Pivovarenko VG, Demchenko AP. Perturbation of planarity as the possible mechanism of solvent-dependent variations of fluorescence quantum yield in 2-aryl-3-hydroxychromones. Spectrochimica Acta Part A 2003;59:787–92. doi:10.1016/S1386-1425(02)00233-0.
[44] Reichardt C. Solvatochromic dyes as solvent polarity indicators. Chem Rev 1994;94:2319–58. doi:10.1021/cr00032a005.
[45] Abraham MH. Hydrogen bonding. 31. Construction of a scale of solute effective or summation hydrogen-bond basicity. J Phys Org Chem 1993;6:660–84. doi:10.1002/poc.610061204.
[46] Klymchenko AS. Solvatochromic and Fluorogenic Dyes as Environment-Sensitive Probes: Design and Biological Applications. Acc Chem Res 2017;50:366–75. doi:10.1021/acs.accounts.6b00517.
[47] Lakowicz JR. Principles of Fluorescence Spectroscopy, 3rd ed.; Springer: New York, NY, 2006, pp. 1–954.
[48] Kenfack CA, Klymchenko AS, Duportail G, Burger A, Mély Y. Ab initio study of the solvent H-bonding effect on ESIPT reaction and electronic transitions of 3-hydroxychromone derivatives. Phys Chem Chem Phys 2012;14:8910. doi:10.1039/c2cp40869d.
[49] Demchenko AP, Tang K-C, Chou P-T. Excited-state proton coupled charge transfer modulated by molecular structure and media polarization. Chem Soc Rev 2013;42:1379–408. doi:10.1039/c2cs35195a.
[50] Skilitsi AI, Agathangelou D, Shulov I, Conyard J, Haacke S, Mély Y, et al. Ultrafast photophysics of the environment-sensitive 4′-methoxy-3-hydroxyflavone fluorescent dye. Phys Chem Chem Phys 2018;20:7885–95. doi:10.1039/c7cp08584b.
[51] Melhuish WH. Quantum Efficiencies of Fluorescence of Organic Substances: Effect of Solvent and Concentration of the Fluorescent Solute. J Phys Chem 1961;65:229–35. doi:10.1021/j100820a009.
[52] Ormson SM, Brown RG, Vollmer F, Rettig W. Switching between charge-and proton-transfer emission in the excited state of a substituted 3-hydroxyflavone. J Photochem Photobiol, A 1994;81:65–72. doi:10.1016/1010-6030(94)03778-7.
[53] Klymchenko AS, Demchenko AP. Multiparametric probing of intermolecular interactions with fluorescent dye exhibiting excited state intramolecular proton transfer. Phys Chem Chem Phys 2003;5:461–8. doi:10.1039/b210352d.
[54] M'Baye G, Klymchenko AS, Yushchenko DA, Shvadchak VV, Ozturk T, Mély Y, et al. Fluorescent dyes undergoing intramolecular proton transfer with improved sensitivity to surface charge in lipid bilayers. Photochem Photobiol Sci 2007;6:71–6. doi:10.1039/b611699j.
[55] Yushchenko DA, Shvadchak VV, Klymchenko AS, Duportail G, Pivovarenko VG, Mély Y. Modulation of excited-state intramolecular proton transfer by viscosity in protic media. J Phys Chem A 2007;111:10435–8. doi:10.1021/jp074726u.
[56] Bilokin MD, Shvadchak VV, Yushchenko DA, Duportail G, Mély Y, Pivovarenko VG. Dual-Fluorescence Probe of Environment Basicity (Hydrogen Bond Accepting Ability) Displaying no Sensitivity to Polarity. J Fluoresc 2009;19:545–53. doi:10.1007/s10895-008-0443-x.
[57] Aso T, Saito K, Suzuki A, Saito Y. Synthesis and photophysical properties of pyrene-labeled 3-deaza-2′-deoxyadenosines comprising a non-π-conjugated linker: fluorescence quenching-based oligodeoxynucleotide probes for thymine identification. Org Biomol Chem 2015;13:10540–7. doi:10.1039/C5OB01605C.
[58] Seidel CAM, Schulz A, Sauer MHM. Nucleobase-specific quenching of fluorescent dyes. 1. Nucleobase one-electron redox potentials and their Correlation with static and dynamic quenching efficiencies. J Phys Chem 1996;100:5541–53. doi:10.1021/jp951507c.
[59] Weatherly SC, Yang IV, Armistead PA, Thorp HH. Proton-coupled electron transfer in guanine oxidation: Effects of isotope, solvent, and chemical modification. Journal of Physical Chemistry B 2003;107:372–8. doi:10.1021/jp022085r.
[60] Seela F, Pujari SS. Azide−Alkyne "Click" Conjugation of 8-Aza-7-deazaadenine-DNA: Synthesis, Duplex Stability, and Fluorogenic Dye Labeling. Bioconjugate Chem 2010;21:1629–41. doi:10.1021/bc100090y.
[61] Huynh MHV, Meyer TJ. Proton-coupled electron transfer. Chem Rev 2007;107:5004–64. doi:10.1021/cr0500030.
[62] Weinberg DR, Gagliardi CJ, Hull JF, Murphy CF, Kent CA, Westlake BC, et al. Proton-coupled electron transfer. Chem Rev 2012;112:4016–93. doi:10.1021/cr200177j.
[63] Luber S, Adamczyk K, Nibbering ETJ, Batista VS. Photoinduced Proton Coupled Electron Transfer in 2-(2′-Hydroxyphenyl)-Benzothiazole. J Phys Chem A 2013;117:5269–79. doi:10.1021/jp403342w.
[64] Pannwitz A, Wenger OS. Photoinduced Electron Transfer Coupled to Donor Deprotonation and Acceptor Protonation in a Molecular Triad Mimicking Photosystem II. J Am Chem Soc 2017;139:13308–11. doi:10.1021/jacs.7b08761.
[65] Choi J, Majima T. Conformational changes of non-B DNA. Chem Soc Rev 2011;40:5893–909. doi:10.1039/c1cs15153c.

Graphical Abstract

To create your abstract, type over the instructions in the template box below.
Fonts or abstract dimensions should not be changed or altered.

Rational design, synthesis, and photophysics of dual-emissive deoxyadenosine analogs

Leave this area blank for abstract info.

H.-N. Le, C. Zilio, G. Barnoin, N.P.F. Barthes, J.-M. Guigonis, N. Martinet , B.Y. Michel, A. Burger